

Combined Use of Proteomic Analysis and Enzyme Activity Assays for Metabolic Pathway Analysis of Glycerol Fermentation by *Klebsiella pneumoniae*

Wei Wang,¹ Jibin Sun,² Michael Hartlep,² Wolf-Dieter Deckwer,¹ An-Ping Zeng²

¹TU-BCE and ²Biochemical Engineering Division, German Research Centre for Biotechnology, Mascheroder Weg 1, 38124 Braunschweig, Germany; telephone: 49-531-6181-188; fax: 49-531-6181-751; e-mail: aze@gbf.de

Received 2 July 2002; accepted 26 February 2003

DOI: 10.1002/bit.10701

Abstract: The fed-batch fermentation of glycerol to 1,3-propanediol by *Klebsiella pneumoniae* displayed an unusual dynamic behavior that can be clearly divided into four distinct phases according to cell growth and CO₂ evolution rate. Metabolism changed significantly during the different phases as reflected by the varied specific rates of substrate consumption and product formation. An assay of activities of the three initial enzymes of glycerol metabolism, namely glycerol dehydratase (GDHt), glycerol dehydrogenase (GDH), and 1,3-propanediol-oxidoreductase (PDOR), showed apparently different patterns of expression. To understand the culture dynamics and patterns of enzyme formation at a more systemic level we analyzed the expression patterns of intracellular proteins of *K. pneumoniae* from different phases of the fed-batch fermentation using two-dimensional gel electrophoresis (2DE). Two new enzymes, namely a phosphoenolpyruvate-dependent dihydroxyacetone kinase (DHAK II) and a hypothetical oxidoreductase (HOR), which are directly related to glycerol metabolism and 1,3-propanediol formation, were identified among the highly expressed proteins. The changes in expression of these new enzymes and several other proteins identified from the 2DE analysis helped to understand not only the dynamic behavior of the fed-batch fermentation reported in this work but also some previously insufficiently understood phenomena related to this fermentation process. In particular, we demonstrated the combined use of proteomic analysis and enzyme activity assay data for metabolic pathway analysis and for a better identification of targets for bioprocess improvement. © 2003 Wiley Periodicals, Inc. *Biotechnol Bioeng* 83: 525–536, 2003.

Keywords: proteomic analysis; pathway analysis; glycerol metabolism; 1,3-propanediol; *Klebsiella pneumoniae*

Correspondence to: A.-P. Zeng

Contract grant sponsors: German Academic Exchange Service (Ph.D. scholarship); European Committee Fifth Framework Project; Deutschen Forschungsgemeinschaft

Contract grant numbers: QLK5-1999-01360; Sonderforschungsbereich 578 (project A5)

INTRODUCTION

Metabolic pathway analysis is an essential part of metabolic engineering. The main objectives of pathway analysis are the estimation of intracellular metabolic fluxes and the identification of limiting metabolic steps. This should then give hints for optimization of bioprocesses either by improving the cell physiology or the genetic composition of the production strains. A prerequisite for pathway analysis is the identification of metabolic pathways involved in a bioprocess. The traditional approach of identifying or finding metabolic pathways for a given microorganism is mainly hypothesis-driven. Hypotheses about metabolism are usually made on the basis of previous knowledge of similar microorganisms and bioprocesses. The hypotheses are then checked by physiological studies and direct enzyme assay. A careful stoichiometric and flux balance analysis of the metabolism can also help to identify pathways as we previously showed for pyruvate metabolism in glycerol fermentation by *Klebsiella pneumoniae* (Menzel et al., 1997; Zeng et al., 1993). The latter has been studied extensively by our group for the microbial production of 1,3-propanediol (for recent reviews, see Biebl et al., 1999; Zeng and Biebl, 2002). 1,3-Propanediol has recently attracted attention as a monomer for a promising new polymer, polytri-methylene terephthalate.

The rapid accumulation of genomic data and fast developments in proteomic analysis have generated much interest in metabolic pathway analysis. The large amount of genomic sequence data make it possible to reconstruct the whole potential metabolic network of an organism (Kanehisa and Goto, 2000; Karp et al., 2000; Ma and Zeng 2002; Overbeek et al., 2000). The analysis of protein expression patterns under experimental conditions given by proteomic analysis can provide much information about functionality and regulation of the metabolic network. This approach to the study of metabolic pathways and their regulation may be called data-driving. The rational and purposeful exploration of this

enormous quantity of genomic and proteomic data for pathway analysis of real bioprocesses is in its infancy, but represents an important area of postgenomic research (Ideker et al., 2001; Seow et al., 2001).

In this work, we demonstrate the unusual dynamics of a fed-batch fermentation of glycerol by *K. pneumoniae*. Results of direct enzyme assays and proteomic analysis of this fermentation process are then presented, which helps to better understand this fermentation process. We demonstrate that the combined use of proteomic analysis and enzyme activity assay is particularly useful for metabolic pathway analysis.

MATERIALS AND METHODS

Organism

Klebsiella pneumoniae DSM 2026 was obtained from the German Collection of Microorganisms (DSMZ).

Medium

Media for anaerobic flask and preculture of *K. pneumoniae* contained (per liter): 20 g glycerol, 3.4 g K_2HPO_4 , 1.3 g KH_2PO_4 , 2 g $(NH_4)_2SO_4$, 0.2 g $MgSO_4 \cdot 7H_2O$, 0.02 g $CaCl_2 \cdot 2H_2O$, 5 mg $FeSO_4 \cdot 7H_2O$, 1 g yeast extract, 2 mL trace elements solution SL7 (Biebl and Pfennig, 1981), and 2 g $CaCO_3$. The fermentation medium for *K. pneumoniae* contained (per liter): 30 g glycerol, 5.35 g NH_4Cl , 0.75 g KCl , 1.38 g $NaH_2PO_4 \cdot H_2O$, 0.28 g Na_2SO_4 , 0.26 g $MgCl_2 \cdot 6H_2O$, 0.42 g citric acid $\cdot H_2O$, 2.9 mg $CaCl_2 \cdot H_2O$, 1 g yeast extract, 0.1 mL desmophen as antifoam agent, and 5 mL trace elements solution. The trace elements solution contained (per liter): 5 g $FeCl_3 \cdot 6H_2O$, 2 g $MnCl_2 \cdot 4H_2O$, 0.684 g $ZnCl_2$, 0.476 g $CoCl_2 \cdot 6H_2O$, 0.17 g $CuCl_2 \cdot 2H_2O$, 62 mg H_3BO_3 , 5 mg $Na_2MoO_4 \cdot 2H_2O$, and 10 mL concentrated HCl (37%).

Fed-Batch Fermentation of Glycerol

Fed-batch fermentations were carried out in a 4-L Setric Bioreactor (Set 4V, Setric Genic Industriel, Toulouse, France) with a starting volume of 2.2 L. The bioreactor was connected to a real-time computer control system (Ubicon, ESD, Hannover, Germany) for on-line data acquisition. The cultivation conditions took place at 37°C, pH 7.0, and 150-rpm agitation. To ensure anaerobic conditions, the bioreactor was sparged with nitrogen at a flow rate of 0.4 volume per volume per minute.

The feeding solution contained 85% glycerol and 0.5% yeast extract. Feeding of substrate was started after consumption of 10 g of alkaline solution (20% NaOH), normally about 4 h after inoculation. Feeding was coupled with alkaline consumption and the feeding factor was about 1.5 to 1.7 g of feed solution per gram of alkaline solution.

Analysis of Biomass, Substrate, and Products

The biomass concentration was measured as absorbance at 650 nm and as dry weight (grams per liter) as well. Glycerol and lactate were assayed enzymatically using test kits from Roche-Biopharm (Darmstadt, Germany). Product concentrations were determined by an isocratic high-performance liquid chromatography (HPLC) system equipped with an HPX-87H column (Bio-Rad) with a differential refractive index detector. As a mobile phase, 0.013N H_2SO_4 with a flow rate of 0.6 mL/min was used at a working temperature of 60°C. Organic acids and ethanol were also determined using gas chromatography equipped with a Chromosorb 101 stainless-steel column (Varian-Chrompack, Frankfurt, Germany) as reported previously (Menzel et al., 1996). Nitrogen was used as carrier gas and *n*-butanol was applied as an internal standard.

Enzyme Assays

Cell free extract for enzyme assay was prepared as described previously (Menzel et al., 1997). The activity of glycerol dehydratase was determined as described by Ahrens et al. (1998). The apparent activity of 1,3-propanediol oxidoreductase was determined using the reverse reaction (1,3-propanediol conversion to 3-hydroxypropionaldehyde), according to Forage and Foster (1982), and a conversion factor of 3.95 for the physiological reaction, according to Ahrens et al. (1998). The activity of glycerol dehydrogenase was measured according to Ruch et al. (1974).

Two-Dimensional Gel Electrophoresis Analysis

After the cells were harvested, they were immediately chilled in ice-water, then centrifuged at 9000 rpm for 30 min at 4°C. Cell pellets were washed twice with phosphate-buffered saline (PBS) and stored at -70°C until use.

To prepare intracellular protein extracts cell pellets were resuspended in 1 mL of lysis buffer containing: 9.5 M urea; 2% (w/v) 3-[(3-cholamidopropyl)-dimethyl-ammonio]-1-propane sulfonate (CHAPS); 0.8% (w/v) Pharmalyte™, pH 3–10; 1% (w/v) dithiothreitol (DTT); and 5 mM Pefabloc (<http://www.weihenstephan.de/blm/deg/manual>). This was disrupted by sonification in an ice bath for 5 × 60 s and additional 2 × 30 s with a 30-s interval between each ultrasonic cycle for an efficient cooling of the sample on ice. A Branson sonifier was used with the amplitude adjusted to 60%. Cell debris were separated by centrifuge at 13,000g for 30 min at 4°C. The total protein concentration in the supernatant was measured with the RCDC Protein Assay Kit (Bio-Rad) according to the manufacturer's instructions. The protein extracts were stored in aliquots at -70°C until two-dimensional (2D) gel electrophoresis.

The first-dimension gel electrophoresis (isoelectric focusing [IEF]) was conducted using the IPGphor Isoelectric Focusing System and Immobiline DryStrip, pH 3–10 NL (both from Amersham Pharmacia Biotech), at a temperature of 20°C. Aliquots of the protein extracts were diluted with

rehydration buffer (8 M urea, 2% [w/v] CHAPS, 0.5% IPG buffer [pH 3 to 10, and 0.28% [w/v] DTT) to adjust the protein concentration to about 1.1 mg/mL. Approximately 500 µg of proteins of each sample (450 µL) were applied to the Immobiline DryStrips for in-gel rehydrations, according to the manufacturer's instructions. During rehydration, low voltages (30 V × 6 h; 60 V × 6 h) were applied for improved sample entry of high-molecular-weight proteins into the polyacrylamide gel (Görg et al., 1999, 2000). Subsequently, IEF was performed with the following parameters: 200 V × 1 h; 500 V × 1 h; 1000 V × 1 h; and gradient from 1000 to 8000 V, within 30 min, then 8000 V × 10 h. Moist filter papers were inserted between the electrodes and the IPG strips to remove small molecules for optimum focusing results (Görg et al., 2000).

The second-dimension gel electrophoresis (sodium dodecylsulfate–polyacrylamide gel electrophoresis [SDS-PAGE]) was carried out using the vertical slab separation unit Ettan Dalt II System, pre-case polyacrylamide gels Ettan Dalt II Gel 12.5%, and the Ettan Dalt II Buffer Kit (all from Amersham Pharmacia Biotech). Before SDS-PAGE, focused IPG strips were equilibrated in 50 mM Tris-HCl (pH 8.8), 6 M urea, 30% (w/v) glycerol, 2% (w/v) SDS containing 1% (w/v) DTT for 15 min, and equilibrated again in the same buffer containing 2.5% iodoacetamide and a trace of bromophenol blue for 15 min (as recommended in the user's manual provided by the manufacturer for Ettan Dalt II Gel 12.5%). The IPG strips were embedded with 0.5% agarose sealing solution and SDS-PAGE separation was performed at 25°C in constant power mode with two running phases: 3 W/gel for 1 h and then 20 W/gel until the bromophenol blue dye front reached the bottom of the gel.

After SDS-PAGE separation, gels were stained with Brilliant Blue G-Colloidal Concentrate (Sigma Co., St. Louis, MO) as follows: gels were fixed in 7% glacial acetic acid plus 40% methanol for 1 h; stained overnight (>15 h) with a staining suspension prepared from the Brilliant Blue G-Colloidal Concentrate according to the manufacturer's suggestion; rinsed with Milli-Q water; and destained with 20% (v/v) methanol until the desired contrast between protein spots and gel background was achieved. Gels can then be stored in 20% ammonium sulfate at 4° to 8°C for several months. For image documentation and computer analysis gels were scanned with a UMAX PowerLook III scanner and UMAX MAGICSCAN software, version 4.4 (UMAX Data Systems, Inc.), at 300-dpi resolution. Computer analysis of the 2D gels for protein spot detection, spot matching between gels, and change of protein expression levels were performed with PHORETIX 2D advanced software, version 5.1 (Phoretix, Newcastle upon Tyne, UK). The molecular weight of individual protein spots was estimated using established 2D SDS-PAGE standards (Bio-Rad). The standards mixture was treated in the same way as for the normal protein samples; for instance, first separation on an IPG strip, and then on a Ettan Dalt II Gel. *pI* values were deduced from the relationship of pH to the percentage length of IPG strips provided by Amersham.

RESULTS AND DISCUSSION

Dynamics of Growth and Metabolism in Fed-Batch Fermentation of Glycerol

Figure 1 shows the results of a fed-batch fermentation of glycerol by *K. pneumoniae*. This fed-batch fermentation exhibited a unusual dynamic behavior that can be divided into four distinct phases according to growth or the evolution of CO₂ in effluent gas (Fig. 1a). In phase I, cells rapidly grew to a relatively high concentration almost without lag phase, and CO₂ production reached a maximum. Thereafter, cells ceased to grow and both biomass concentration and CO₂ production reached a minimum (phase II). In phase III, cells again grew and CO₂ production reached a second maximum. In phase IV, CO₂ production declined continuously and biomass concentration remained relatively constant. These varied phases of cell growth and CO₂ production were also reflected in the product formation (Fig. 1b). In phase I, only 1,3-propanediol was produced in a significant amount. Its production rate was reduced in subsequent phases, especially phases II and IV. The formation of acetate, lactate, and ethanol was accelerated in phases II to IV. These results indicate a change in cell physiology and metabolism in the different phases as evidenced by the changes in specific rates of substrate uptake and product formation (Fig. 2). We found that the specific formation rate of lactate increased significantly in phase 2 and reached its maximum at the end of this phase. After the onset of decline in lactate formation, the formation rate of ethanol increased markedly

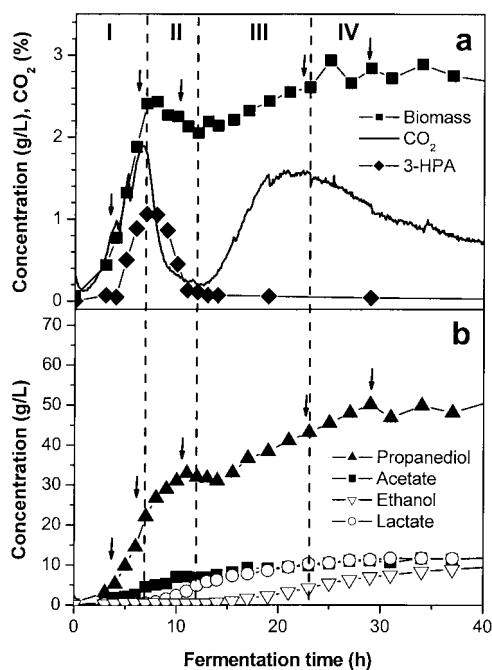


Figure 1. Time course of cell growth and product formation in fed-batch fermentation of glycerol by *Klebsiella pneumoniae*. Arrows indicate sampling time for 2D proteomic analysis. The fermentation is divided into four phases (I to IV) according to cell growth and CO₂ evolution rate.

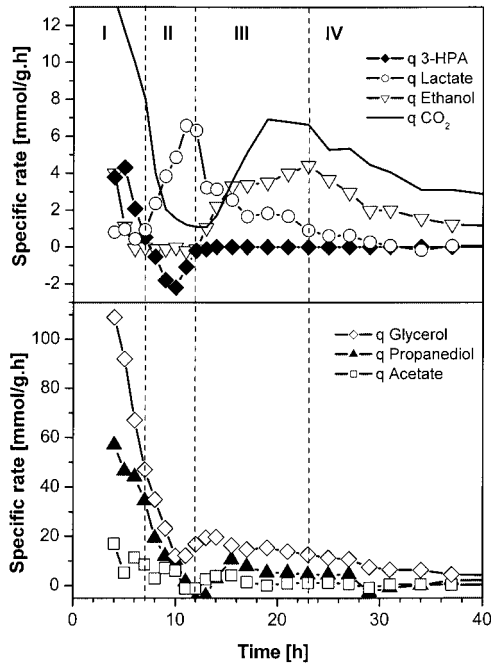


Figure 2. Specific rates of substrate consumption and product formation in the different phases of fed-batch fermentation.

in phase III, and reached its maximum in the transition from phase III to phase IV.

The reason(s) for the observed changes of cell growth and metabolism in this fermentation process is not clear. In fact, a similar phenomenon was reported only recently (Hartlep et al., 2002). Hartlep et al. (2002) termed this phenomenon “metabolic switching,” and hypothesized that the accumulation of acetate (to a critical level of about 6 to 10 g/L) may be one of the triggers for this switching. This critical level of acetate was reached around the transition from phase I to phase II in the fed-batch fermentation (Fig. 1a). In this study, we observed a significant accumulation of the intermediate 3-hydroxypropionaldehyde (3-HPA) in the first phase (Fig. 1a), which was then reconsumed in the second

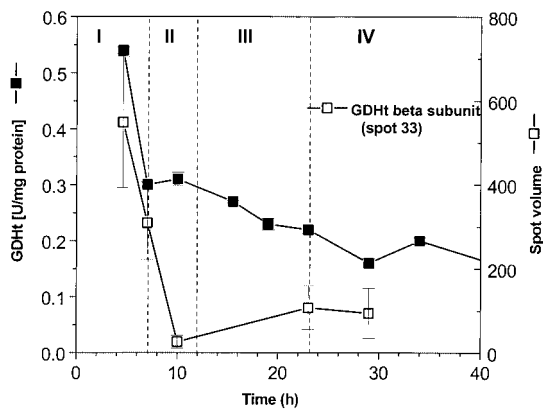


Figure 3. Specific activity of GDHt by enzyme assay. Also shown is the normalized spot volume of spot 33 on 2D gel identified as the β subunit of GDHt.

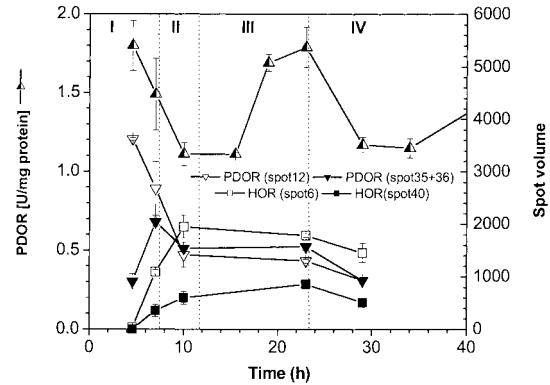


Figure 4. Apparent specific activity of PDOR by enzyme assay. Also shown are the normalized spot volumes of spots 12, 35, and 36 on the 2D gel, which were identified as isoforms of PDOR, and normalized spot volumes of spots 6 and 40, which were identified as isoforms of a hypothetical oxidoreductase (HOR), a second enzyme that is hypothesized to catalyze the same reaction as PDOR.

phase. It is known that 3-HPA is very toxic to the growth of many microorganisms (Barbirato et al., 1996). It is possible that the accumulation of 3-HPA caused the metabolic switch from phase I to phase II. The reconsumption of 3-HPA allowed the cells to grow again (switching to phase III). Switching from phase III to phase IV may be due to the accumulation of other major fermentation products (1,3-PD, lactate, and ethanol).

Assay of Activities of Key Enzymes for Glycerol Metabolism

To understand the reasons for metabolic switching and regulation at the enzyme level we measured the in vitro activities of the first three enzymes of anaerobic glycerol metabolism. These included: glycerol dehydratase (GDHt), which catalyzes the conversion of glycerol to 3-HPA; apparent 1,3-propanediol oxidoreductase (PDOR), which catalyzes the formation of 1,3-PD from 3-HPA; and glycerol

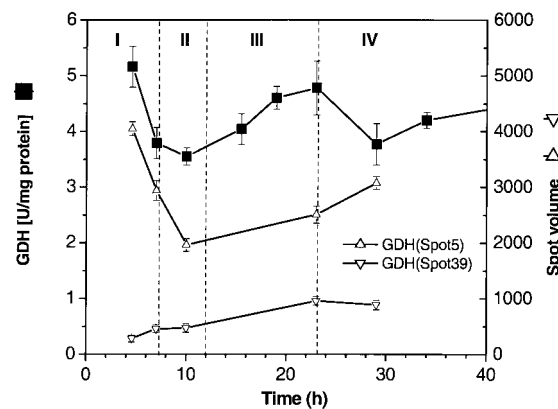


Figure 5. Specific activity of GDH by enzyme assay. Also shown are the normalized spot volumes of spots 5 and 39 on the 2D gel, which were identified as two isoforms of GDH.

dehydrogenase (GDH), which catalyzes the oxidative conversion of glycerol to dihydroxyacetone (DHA). The latter is then channeled into the glycolysis pathways for the generation of energy and reducing power. The specific activities of these enzymes are shown in Figures 3 to 5. For these three enzymes, expression decreased significantly in phase I. This may be due to the necessity of avoiding further accumulation of the toxic intermediate 3-HPA. In general, the *in vitro* activity of GDHt was much lower than those of PDOR and GDH throughout the fermentation, supporting the aforementioned hypothesis concerning 3-HPA formation.

The specific activities of all the enzymes continued to decrease in phase II. In accordance with the renewed growth the specific activities of PDOR and GDH increased significantly in phase III, whereas the activity of GDHt further decreased in phase III and remained relatively constant in phase IV. In phase IV, the activities of PDOR and GDH again decreased. Thus, except for GDHt, the changes in expression of PDOR and GDH appeared to have the same pattern as the cell growth and product formation. The differing behavior of GDHt, PDOR, and GDH was not expected because the genes coding for these enzymes all belong to the same regulon (*dha*) and should therefore be regulated by the same inducers or repressors (Forage and Lin, 1982). In particular, the specific activities of GDHt and PDOR would be expected to change in a similar manner because they catalyze the two successive reactions of the reductive pathway of glycerol utilization.

Although the activities of the three enzymes measured by

direct enzyme assay are informative, they give a rather limited picture about the regulation of glycerol metabolism, especially with regard to the unusual dynamic behavior of cell growth and metabolism shown in Figures 1 and 2. For a better understanding of these phenomena at a more global level, and particularly for explaining the different expression patterns among GDHt, PDOR, and GDH, we analyzed the protein expression patterns in the four different fermentation phases using 2D gel electrophoresis analysis.

Proteomic Analysis of *K. pneumoniae* From Glycerol Fermentation

Samples from the fed-batch fermentation were taken at the timepoints indicated in Figure 1 for proteomic analysis of *K. pneumoniae*. Figure 6 shows the typical protein expression pattern of *K. pneumoniae* obtained from 2D gel electrophoresis using the Immobiline DryStrip (pH 3 to 10 NL) for the first-dimensional separation. We chose this Immobiline DryStrip with a nonlinear pH gradient to facilitate better resolution between pH 5 and 7, where most of the proteins appeared, and also to obtain a complete image of the protein extract of *K. pneumoniae*. After Coomassie staining, 173 to 214 spots were detected on different gels using the 2D evaluation. Each sample was measured twice. To compensate for gel staining variations and differences in protein spot numbers for each gel, normalized spot volumes were used for comparison of protein expression levels. The normalized spot volume was calculated as single spot volume divided by the total spot volume and then multiplied by total

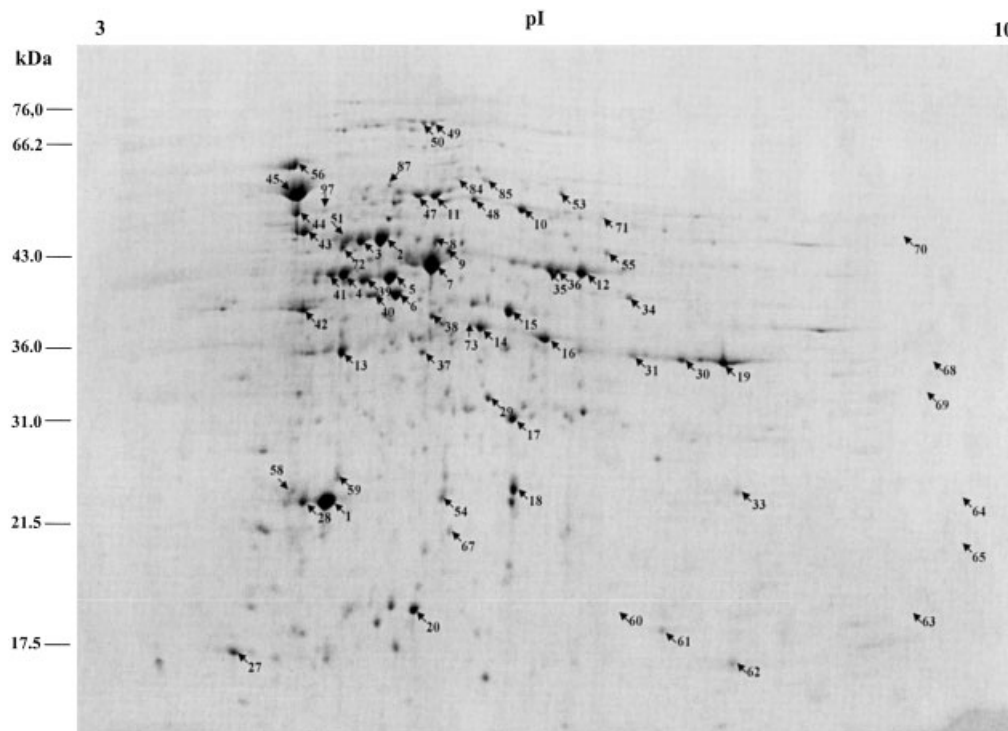


Figure 6. Typical image of 2DE gel electrophoresis analysis of intracellular proteins of *K. pneumoniae* grown on glycerol (23 h after inoculation of culture; Fig. 1).

Table I. Proteins identified with in-gel digestion and MALDI/TOF-MS and/or ESI/MS_MS analysis.

Function category	Spot no. ^a	Annotation and/or homologue proteins	pI ^c	Mw ^c (kDa)	
Carbohydrate metabolism (<i>dha</i> regulon related)	5	Glycerol dehydrogenase (EC 1.1.1.6) (GLDH), P45511	5.31	41.4	
	39	GLDA_CITFR ^b	5.23	41.2	
	97	Dihydroxyacetone kinase I (EC 2.7.1.29), sp P45510 DAK_CITFR	5.03	52.0	
	42	Dehydroxyacetone kinase II, subunit 1 (EC 2.7.1.121), P76015 YCGT_ECOLI	4.91	39.1	
	18	Dihydroxyacetone kinase II, subunit 2 (EC 2.7.1.121), P76014 YCGS_ECOLI	5.70	24.8	
	33	Glycerol dehydratase β subunit (EC 4.2.1.30), tr O08505	6.72	24.3	
	62	Glycerol dehydratase α subunit (EC 4.2.1.30), tr Q59475	6.66	16.8	
	12	1,3-propanediol dehydrogenase (EC 1.1.1.202), Q59477	5.91	41.8	
	35	DHAT_KLEPN	5.81	42.0	
	36		5.84	41.8	
	6	Hypothetical oxidoreductase yqhD (EC 1.1.-.-), Q46856	5.32	40.2	
	40	YQHD_ECOLI	5.25	40.1	
	Glycolysis/gluconeogenesis	87	Phosphoglucosmutase (EC 5.4.2.2) (Glucose phosphomutase) (PGM), sp P36938 PGMU_ECOLI	5.30	57.2
		15	Fructose-bisphosphate aldolase class II (EC 4.1.2.13), P11604 ALF_ECOLI	5.69	39.0
17		Triosephosphate isomerase (EC 5.3.1.1) (TIM), Q9Z6B9 TPIS_ENTCL	5.70	31.5	
19		Glyceraldehyde 3-phosphate dehydrogenase (EC 1.2.1.12), P06977 G3P1_ECOLI	6.57	35.5	
30			6.25	35.6	
31			6.07	35.9	
4		Phosphoglycerate kinase (EC 2.7.2.3), Q8XG18 PGK_SALTY	5.14	41.6	
41			5.07	41.6	
29		Phosphoglycerate mutase 1 (EC 5.4.2.1), P31217 PMG1_ECOLI	5.62	32.3	
2		Enolase (EC 4.2.1.11), P08324 ENO-ECOLI	5.28	46.5	
3			5.22	46.1	
51			5.17	45.9	
85		Pyruvate kinase I (EC 2.7.1.40), sp P77983 KPY1_SALTY	5.61	58.4	
84		5.52	58.7		
One-carbon metabolism	72	S-adenosylmethionine synthetase (EC 2.5.1.6), P04384 METK_ECOLI	5.13	44.9	
Phosphate metabolism	58	Inorganic pyrophosphatase (EC 3.6.1.1), Q8XGI0 IPYR_SALTY	4.86	24.3	
Energy metabolism	10	ATP synthase α chain (EC 3.6.3.14), P00822 ATPA_ECOLI	5.72	52.5	
	48		5.58	54.5	
	43	ATP synthase β chain (EC 3.6.3.14), P00824 ATPB_ECOLI	4.92	48.0	
	69	ATP synthase γ chain (EC 3.6.3.14), P00837 ATPG_ECOLI	8.55	33.1	
Amino acid metabolism	8	Argininosuccinate synthase (EC 6.3.4.5), P22767 ASSY_ECOLI	5.44	46.0	
	9	Threonine synthase (EC 4.2.3.1), P00934 THRC_ECOLI	5.48	43.8	
	37	2,3,4,5-tetrahydropyridine-2-carboxylate <i>N</i> -succinyltransferase, P03948 DAPD_ECOLI, P41397 DAPD-KLEPN	5.40	36.1	
	16	Cysteine synthase A (EC 4.2.99.8), P11096 CYSK_ECOLI	5.79	37.1	
	14		5.60	37.8	
	55	Serine hydroxymethyltransferase (EC 2.1.2.1), P06192 GLYA_SALTY	5.99	43.3	
Protein biosynthesis	7	Elongation factor TU (EF-TU), EFTU_SALTY, P21694	5.43	42.4	
	13	Elongation factor Ts (EF-Ts), Q8XGS0 EFTS_SALTY	5.13	36.2	
	44	Trigger factor (TF), Q8XFC4 TIG_SALTY	4.87	51.8	
	64	50S ribosomal protein L6, P02390 RL6_ECOLI	8.84	24.0	
	61	50S ribosomal protein L9, Q8Z163 RL9_SALTI	6.16	17.9	
	63	50S ribosomal protein L10 (L8), P17352 RL10_SALTY	8.50	18.5	
27	50S ribosomal protein L7/L12 (L8), P18081 RL7_SALTY	4.53	17.2		
DNA replication, recombination, and repair	54	Single-strand binding protein (SSB), P02339 SSB_ECOLI	5.47	23.9	
	56	Chaperone protein DnaK (heat shock protein), Q8Z9R1 DNAK_SALTI	4.84	61.7	

Table I. Continued

Function category	Spot no. ^a	Annotation and/or homologue proteins	pI ^c	Mw ^c (kDa)
Membrane transport	53	Periplasmic oligopeptide-binding protein precursor, P23843 OPPA_ECOLI	5.85	55.8
	71	Periplasmic dipeptide transport protein precursor, P23847 DPPA_ECOLI	5.97	50.7
	70	Putative binding protein yLiB precursor, P75797 YLIB-ECOLI	8.20	48.5
	73	Glycine betaine-binding periplasmic protein precursor, P14177 PROX_ECOLI	5.56	38.0
Stress proteins	20	10 kDa chaperonin (protein Cpn10) (groES protein), P05380 CH10_ECOLI	5.38	18.6
	45	60 kDa chaperonin (protein Cpn60) (groEL protein), (HSP60KP), O66026 CH60_KLEPN	4.87	55.9
	34	<i>N</i> -ethylmaleimide reductase (EC 1.-.-.), P77258 NEMA_ECOLI	6.06	39.9
	1	Alkyl hydroperoxide reductase C22 protein (EC 1.6.4.-), P19479 AHPC_SALTY	5.05	23.4
	28	P19479 AHPC_SALTY	4.92	23.4
	11	Alkyl hydroperoxide reductase subunit F (EC 1.6.4.-), P19480 AHPF_SALTY	5.44	55.5
	47	AHPF_SALTY	5.39	55.3
	59	Probable peroxiredoxin, P57279 TSAA_BUCAI	5.11	25.8
	Uncategorized	38	Outer membrane protein A precursor, P24017 OMPA_KLEPN	5.43
49		CLPB protein (heat shock protein F84.1), P03815 CLPB_ECOLI	5.43	72.4
50		CLPB_ECOLI	5.41	72.4
60		Protein yifE, P27827 YIFE-ECOLI	5.93	17.9
67		Protein yajQ, P77482 YAJQ-ECOLI	5.49	21.1
68		Protein ydgH precursor, P76177 YDGH-ECOLI	8.59	35.5
65		Histone-like protein HLP-1 precursor, P11457 HHPA-ECOLI	8.82	20.8
66		Protein ygbA, P25728 YGBA_ECOLI	7.79	16.5

^aRefers to the protein numbering in Figure 6.

^bProtein index from Swiss-Prot or TrEMBL.

^cpI and Mw estimated from 2DE results.

spot area. Differences in the normalized spot intensities between the two measurements were <20% for most of the proteins depicted in Figures 3 to 5.

More than 190 spots (62 indicated in Fig. 6) were excised from the gels for protein identification by peptide mass fingerprinting with matrix-assisted laser desorption ionisation time-of-flight mass spectrometry (MALDI-TOF MS). Some of the spots were also subjected to partial peptide sequencing with electrospray ionisation quadrupole-time-of-flight tandem mass spectrometry (ESI-Qq TOF MS/MS). Some spots marked were almost invisible in this gel, but appeared clearly on gels of samples from the early fermentation stage. There were 163 spots identified as 122 proteins and their isoforms by the combined use of MS data and genome data of *K. pneumoniae* as described in detail by Wang et al. (2003). The proteins identified can be classified into several function categories as briefly summarized in Table I for the spots indicated in Figure 6. Examples of proteins for these function categories are shown schematically in Figure 7, which illustrates the major metabolic pathways of glycerol fermentation. These include all three known enzymes of the *dha* regulon just mentioned (PDOR, GDH, and two of the three subunits of GDHt) and two new enzymes related directly to the anaerobic metabolism of glycerol. One of these new enzymes is dihydroxyacetone kinase II (DHAK II) with its two subunits. Unlike the known ATP-dependent dihydroxyacetone kinase (DHAK I)

in *K. pneumoniae* (Johnson et al., 1984) and *Citrobacter freundii* (Daniel et al., 1995), DHAK II is a PEP-dependent *dha* kinase (Gutknecht et al., 2001). Its presence in *K. pneumoniae* and its PEP dependency was first suggested by a comparative genome analysis of genes related to the *dha* regulon and confirmed by in vitro enzyme activity assay (Sun et al., 2002). It is noteworthy that DHAK I, which has so far been considered responsible for the conversion of dihydroxyacetone (DHA) to dihydroxyacetone phosphate (DHAP) in glycerol fermentation, had a much lower expression level than DHAK II throughout the fermentation.

The second new enzyme is a hypothetical oxidoreductase (HOR) that appeared as two isoforms on the 2DE gel (spots 6 and 40 in Fig. 6). Because of its importance in the production of 1,3-propanediol we examined the function annotation of this protein in some more detail. As shown in Figure 8 by protein sequence alignment, the amino acid sequence of this protein is 89% identical to the hypothetical oxidoreductase of *E. coli* (*YqhD*), 38% identical to the NADH-dependent butanol dehydrogenase A of several bacteria, and 25% identical to the PDOR of *C. freundii* and *K. pneumoniae*. The HOR of *E. coli* was confirmed to be able to replace the function of PDOR in *E. coli* (Emptage et al., 2001). *E. coli*, which does not contain any native genes of the *dha* regulon, can produce a large amount of 1,3-propanediol after transformation with most of the *dha* regulon genes of *K. pneumoniae*, except the gene for PDOR

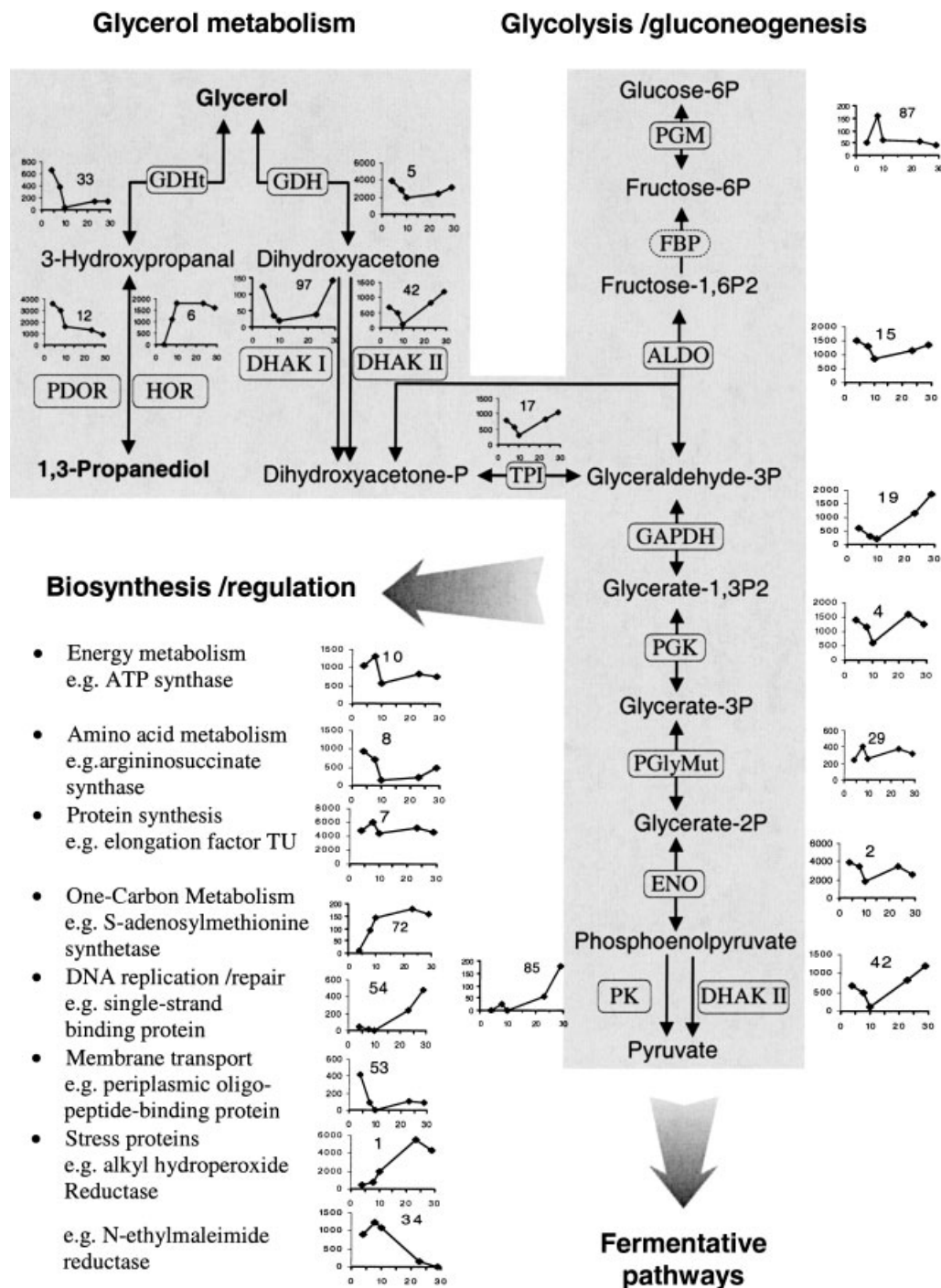


Figure 7. Schematic presentation of identified proteins (enzymes) and their functions related to the metabolism of glycerol and biosynthesis. Also shown are the expression change patterns of these proteins during fed-batch fermentation.

(*dhaT*). Interestingly, such transformants can produce even much higher amounts of 1,3-propanediol than strains transformed with the whole *dha* regulon, including *dhaT*. When the native gene *yqhD* was disrupted, the high producer completely lost its ability to produce 1,3-propanediol, proving that YqhD is directly responsible for reducing 3-HPA to 1,3-propanediol in the recombinant *E. coli* strain. Thus, spots 6 and 40 on the 2D gel of *K. pneumoniae*, which are very similar to YqhD, are annotated as a hypothetical 1,3-

propanediol oxidoreductase in *K. pneumoniae* and classified as “*dha*-regulon-related” proteins. Additional evidence for the existence of enzyme(s) other than PDOR for the formation of 1,3-propanediol in *K. pneumoniae* came from a comparison of changes of PDOR determined by both 2D-gel analysis and its directly measured apparent activity by enzyme assay (Fig. 4; see discussion in what follows).

The second functional category contains enzymes for glycolysis and gluconeogenesis (Fig. 7), including triosephos-

phate isomerase (TPI), fructose-bisphosphate aldolase class II (ALDO), glyceraldehyde 3-phosphate dehydrogenase (GAPDH), phosphoglycerate kinase (PGK), phosphoglycerate mutase 1 (PglyMut), and enolase (EDO). PEP-dependent DHAK II also contributes to this pathway by converting phosphoenolpyruvate (PEP) to pyruvate. These enzymes channel dihydroxyacetone phosphate from glycerol dissimilation into glycolysis and gluconeogenesis pathways, which play key roles in the central metabolism by generating ATP, reducing power, and metabolic intermediates. Thus, these enzymes are among the most frequently expressed proteins in glycerol fermentation. Several proteins involved in biosynthesis, transport, and stress responses are also included in Figure 7.

Use of Proteomic Data and Enzyme Activity Assay for Analysis of Glycerol Fermentation

The dynamics of protein expression patterns is shown with an enlarged section of the 2D-gel images in time series in Figure 9, and shown schematically with the metabolic pathways in Figure 7. As demonstrated by the four spots in Figure 9, the pattern of protein expression changed significantly during the first 30 h of fermentation. Enzyme DHAK II (spots 42 and 18) represents proteins having an expres-

sion that first decreased significantly during the first two phases of the fermentation, but increased in later phases. This pattern of change in protein expression was similar to the growth of cells in phases II to IV (Figure 1). Several proteins for glycolysis, such as triosephosphate isomerase (spot 17) and glyceraldehyde phosphate dehydrogenase (spot 19), followed the same pattern. PDOR (spot 12) represents proteins having an expression that decreased continuously during fermentation. Except for enzymes PDOR and GDHt, some membrane transport proteins, such as periplasmic oligopeptide-binding protein (spot 53), and some ribosomal proteins, such as the 50S ribosomal protein L9 (spot 61), also belong in this category. HOR (spot 6) represents a group of identified proteins having an expression that increased from a very low level in phase I to a relatively high level in phase IV. Specifically this group includes the DNA repair protein (spot 54) and the alkyl hydroperoxide reductases (spots 1, 28, 11, and 47). These proteins are involved in overcoming stress conditions, indicating physiological stress in the late phases of fed-batch fermentation. The strongly increased formation of HOR, especially during phases I and II of the fermentation, may also be physiologically interpreted as a means to protect against stress or toxic conditions caused by a possible ac-

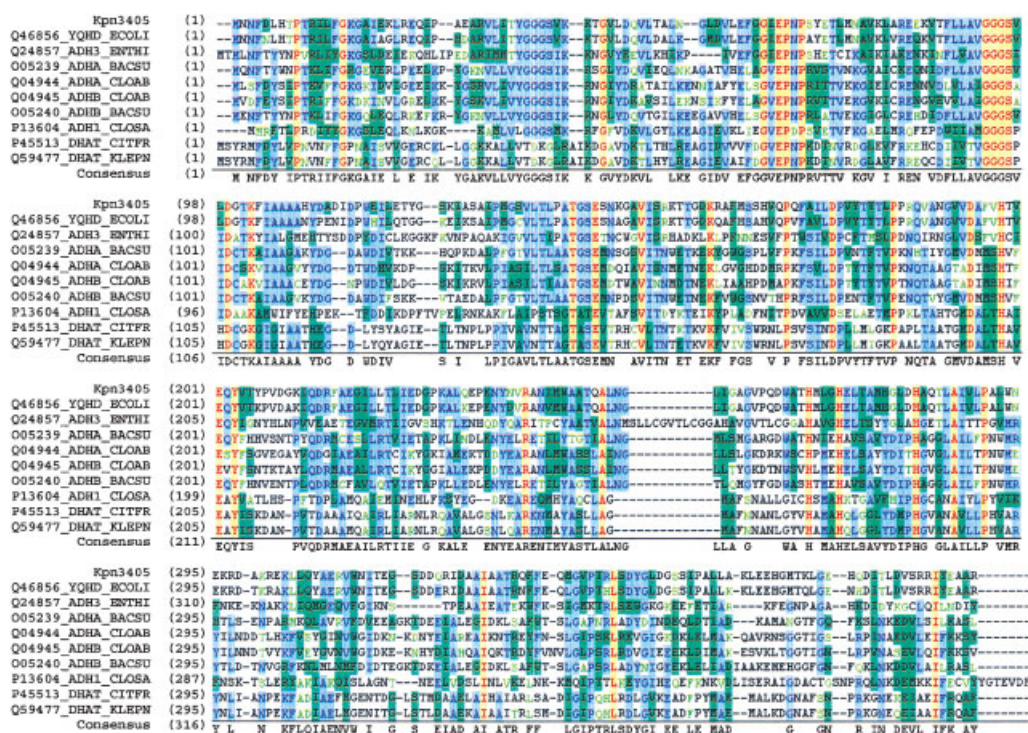


Figure 8. Protein sequence alignments of a newly identified putative 1,3-propanediol oxidoreductase (Kpn3405) of *K. pneumoniae* with similar proteins in Swiss-Prot: Q46856_YQHD_ECOLI, hypothetical oxidoreductase YqhD of *E. coli*; Q24857_ADH3_ENTHI, alcohol dehydrogenase 3 of *Entamoeba histolytica*; O05239_ADHA_BACSU, probable NADH-dependent butanol dehydrogenase 1 of *Bacillus subtilis*; Q04944_ADHA_CLOAB, NADH-dependent butanol dehydrogenase A of *Clostridium acetobutylicum*; Q04945_ADHB_CLOAB, NADH-dependent butanol dehydrogenase B of *C. acetobutylicum*; O05240_ADHB_BACSU, probable NADH-dependent butanol dehydrogenase 2 of *Bacillus subtilis*; P13604_ADH1_CLOSA, NADPH-dependent butanol dehydrogenase of *Clostridium saccharobutylicum*; P45513_DHAT_CITFR, 1,3-propanediol oxidoreductase of *Citrobacter freundii*; and Q59477_DHAT_KLEPN, 1,3-propanediol oxidoreductase of *K. pneumoniae*. The identities between Kpn3405 and the aforementioned proteins are 88.9%, 37.4%, 37.8%, 37.5%, 35.6%, 37.7%, 21.1%, 24.8%, and 24.6%, respectively.

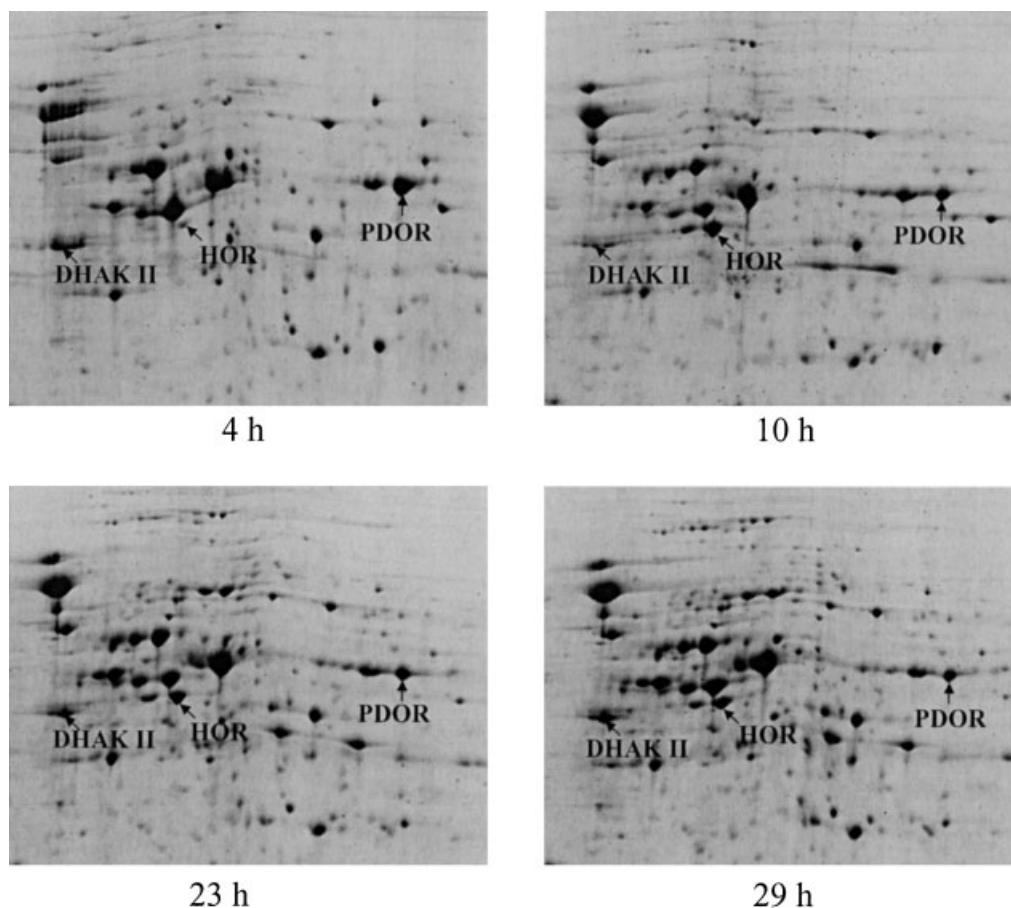


Figure 9. Changes of protein expression measured by 2D gel electrophoresis as function of fermentation time.

cumulation of 3-HPA. As shown by Ahrens et al. (1998), PDOR from *K. pneumoniae* has a relatively high reaction activity for the reverse directions in the conversion of 3-HPA to 1,3-PD, resulting in a potentially large accumulation of 3-HPA in the later phase of fermentation, when the concentration of 1,3-PD is quite high (Fig. 1). However, it is known that the activity of butanol dehydrogenase (BuDH) from *Clostridium acetobutyricum*, which was well characterized (Walter et al., 1992; Youngleson et al., 1989) and has a high protein sequence identity to HOR, is 50-fold lower in the reverse direction compared with the forward direction in (Welch et al., 1989). As mentioned earlier, the HOR from *E. coli* showed properties similar to those of BuDH. Thus, the involvement of HOR in the formation of 1,3-PD may reduce the accumulation of 3-HPA and the stress for cell growth, causing the metabolism switch from phase II to phase III.

We have demonstrated that proteomic analysis can provide useful information about metabolic regulation as it relates to the dynamics observed in the fed-batch fermentation process. In what follows, we further show the importance of combining data from the proteomic analysis and the direct enzyme activity assay for improving our understanding of glycerol fermentation.

In previous work (Menzel et al., 1998) the enzyme ac-

tivities and fluxes of pyruvate metabolism in the glycerol fermentation were determined. It was observed that pyruvate kinase that catalyzes the conversion of PEP to pyruvate (Fig. 7) had a much lower activity compared with the upstream enzymes (e.g., GDH) of glycerol assimilation (Ahrens et al., 1998) and the downstream enzymes (such as pyruvate formate-lyase), suggesting that pyruvate kinase (PK) may be one of the limiting enzymes in glycerol fermentation. Another interesting and somewhat surprising observation by Menzel et al. (1998) was that the ratio of in vitro to in vivo activities of PK was in some cases clearly <1 (around 0.8 to 0.9). This represents an unrealistic value because the in vitro-measured maximum activity of the enzyme should theoretically not be lower than the in vivo-measured activity. This seemingly unrealistic ratio of in vitro to in vivo activities of PK can now be understood in view of the finding with PEP-dependent dihydroxyacetone kinase (DHAK II). This enzyme catalyzes at the same time as the conversion of PEP to pyruvate. As shown in Figure 7, the expression level of DHAK II was much higher than that of PK, especially in the first two phases of the fermentation. Because it was DHAK II, not PK, that was identified among the most highly expressed spots on the 2D gels, it is reasonable to assume a significant contribution of DHAK II to the formation of pyruvate. If the flux from PEP to pyruvate

catalyzed by DHAK II is subtracted in the calculation of the in vivo activity of PK, then the ratio of in vitro to in vivo activities for this enzyme would thus be >1.0. Therefore, proteomic analysis explained the seemingly controversial results concerning the pyruvate metabolism. It can also be better understood why the activity of PK is much lower than in other enzymes in the related pathways. In this context, we can also state that proteomic analysis is useful for identifying real targets for metabolic engineering of production strains. In the case of glycerol conversion to 1,3-propanediol, an overexpression of the previously assumed limiting enzyme, pyruvate kinase, will obviously not lead to significant improvement of the process because it does not represent a limiting step according to the proteomic analysis in this study.

Another noteworthy finding from the proteomic analysis pertains to the conversion of 3-HPA to 1,3-propanediol, a key step in the fermentation process (Fig. 7). Figures 3 to 5 show comparisons of changes in the in vitro activities from the enzyme assay and the changes of expression levels determined from 2DE analysis for three of the *dha* regulon enzymes. For GDHt (spot 33) and GDH (spot 5) the general patterns of changes are quite similar. However, a clear discrepancy was found for the assumed specific activity of PDOR in Figure 4. None of the changes in the spots identified as isoforms of PDOR can explain the significant increase in the in vitro enzyme activity measured in phase III of the fermentation. This implies that other enzyme(s) may be responsible for the increased in vitro activity. Indeed, the 2D analysis identified a protein (HOR) (spots 6 and 40 as isoforms in Fig. 6) that can catalyze the conversion of 3-HPA to 1,3-propanediol. The expression of HOR needed an induction and increased significantly after a fermentation time of about 7 to 10 h (phase II, Fig. 4). It remained relatively constant in phase III and decreased slightly in phase IV. Thus, the induced expression of HOR may only partially explain the observed renewed increase in enzyme activity and metabolic flux for the conversion of 3-HPA to 1,3-propanediol during the third phase of the fed-batch fermentation (Fig. 2). It would be of interests to examine whether other enzymes, such as alkyl hydroperoxide reductase (spot 1), which increased significantly on the 2D gel in phase III (Fig. 7), could also catalyze the conversion of 3-HPA to 1,3-propanediol.

In conclusion, proteomic analysis provides a wealth of information on the regulation of metabolic pathways in glycerol fermentation. For a more exhaustive exploration of this approach, a more systematic study under varied experimental conditions, preferably with directed physiological or genetic perturbation of the metabolic and regulatory networks, is desirable (Ideker et al., 2001). For this purpose, we have recently established a method to knock out selected genes in *K. pneumoniae*, which will be used to characterize the new enzymes, DHAK II and HOR, reported in this work.

References

- Ahrens K, Menzel K, Zeng AP, Deckwer WD. 1998. Kinetic, dynamic, and pathway studies of glycerol metabolism by *Klebsiella pneumoniae* in anaerobic continuous culture. Part III: Enzymes and fluxes of glycerol dissimilation and 1,3-propanediol formation. *Biotechnol Bioeng* 59: 544–552.
- Altschul SF, Madden TL, Schaffer AA, Zhang J, Zhang Z, Miller W, Lipman DJ. 1997. Gapped BLAST and PSI-BLAST: A new generation of protein database search programs. *Nucl Acids Res* 25:3389–3402.
- Barbarito F, Grivel JP, Soucaille P, Bories A. 1996. 3-Hydroxypropionaldehyde, an inhibitory metabolite of glycerol fermentation to 1,3-propanediol by enterobacterial species. *Appl Environ Microbiol* 62: 1448–1451.
- Biebl H, Menzel K, Zeng AP, Deckwer WD. 1999. Microbial production of 1,3-propanediol. *App Microbiol Biotechnol* 52:289–297.
- Daniel R, Stuert K, Gottschalk G. 1995. Biochemical and molecular characterization of the oxidative branch of glycerol utilization by *Citrobacter freundii*. *J Bacteriol* 177:4392–4401.
- Emptage M, Haynie S, Laffend L, Pucci J, Whited G. 2001. Process for the biological production of 1,3-propanediol with high titer. E. I. du Pont de Nemours and Co. and Genencor International, Inc. U.S. patent WO 01/12833 A2.
- Forage RG, Foster MA. 1982. Glycerol metabolism in *Klebsiella pneumoniae*: Functions of the coenzyme B12-dependent glycerol and diol dehydratase. *J Bacteriol* 149:413–419.
- Forage RG, Lin ECC. 1982. *dha* systems mediating aerobic and anaerobic dissimilation of glycerol in *Klebsiella pneumoniae* NCIB418. *J Bacteriol* 151:591–599.
- Görg A, Obermaier C, Boguth G, Harder A, Scheibe B, Wildgruber R, Weiss W. 2000. The current state of two-dimensional electrophoresis with immobilized pH gradients. *Electrophoresis* 21:1037–1053.
- Görg A, Obermaier C, Boguth G, Weiss W. 1999. Recent developments in two-dimensional gel electrophoresis with immobilized pH gradients: Wide pH gradients up to pH 12, longer separation distances and simplified procedures. *Electrophoresis* 20:712–717.
- Gutknecht R, Beutler R, Garcia-Alles LF, Baumann U, Erni B. 2001. The dihydroxyacetone kinase of *Escherichia coli* utilizes a phosphoprotein instead of ATP as phosphoryl donor. *EMBO J* 20:2480–2486.
- Hartlep H, Hussmann W, Prayitno N, Meynial-Salles I, Zeng AP. 2002. Study of two-stage processes for the microbial production of 1,3-propanediol from glucose. *Appl Microbiol Biotechnol* 60:60–66.
- Ideker T, Thorsson V, Ranish JA, Christmas R, Buhler J, Eng JK, Bumgarner R, Goodlett DR, Aebersold R, Hood L. 2001. Integrated genomic and proteomic analysis of a systematically perturbed metabolic network. *Science* 292:929–934.
- Johnson EA, Burke SK, Forage RG, Lin ECC. 1984. Purification and properties of dihydroxyacetone kinase from *Klebsiella pneumoniae*. *J Bacteriol* 160:55–60.
- Kanehisa M, Goto S. 2000. KEGG: Kyoto encyclopedia of genes and genomes. *Nucl Acids Res* 28:27–30.
- Karp PD, Riley M, Saier M, Paulsen IT, Paley SM, Pellegrini-Toole A. 2000. The EcoCyc and MetaCyc databases. *Nucl Acids Res* 28:56–59.
- Ma HW, Zeng AP. 2002. Reconstruction of metabolic networks from genome data and analysis of their global structure for various organisms. *Bioinformatics* 19:270–277.
- Menzel K, Ahrens K, Zeng AP, Deckwer WD. 1998. Kinetic, dynamic and pathway studies of glycerol metabolism by *Klebsiella pneumoniae* in anaerobic continuous culture, Part IV: Enzymes and fluxes of pyruvate metabolism. *Biotechnol Bioeng* 60:617–626.
- Menzel K, Zeng AP, Deckwer WD. 1997. Enzymatic evidence of involvement of pyruvate dehydrogenase in anaerobic glycerol metabolism by *Klebsiella pneumoniae*. *J Biotechnol* 56:135–142.
- Overbeek R, Larsen N, Pusch G, D'Souza M, Selkov E, Kyrpides N, Fonstein M, Maltsev N, Selkove E. 2000. WIT: Integrated system for high-throughput genome sequence analysis and metabolic reconstruction. *Nucl Acids Res* 28:123–125.

- Ruch FE, Lengeler J, Lin ECC. 1974. Regulation of glycerol catabolism in *Klebsiella aerogenes*. *J Bacteriol* 119:50–56.
- Seow TK, Korke R, Liang RCMY, Ong SE, Ou K, Wong K, Hu WS, Chung MCM. 2001. Proteomic investigation of metabolic shift in mammalian cell culture. *Biotechnol Progr* 17:1137–1144.
- Sun J, van den Heuvel J, Soucaille P, Qu Y, Zeng AP. 2003. Comparative genomic analysis of *dha* regulon and related genes for anaerobic glycerol metabolism in bacteria. *Biotechnol Progr* 19:263–272.
- Walter KA, Bennett GN, Papoutsakis E. 1992. Molecular characterization of two *Clostridium acetobutyricum* ATCC 824 butanol dehydrogenase isozymes genes. *J Bacteriol* 174:7149–7158.
- Wang W, Sun J, Zeng AP, Deckwer WD. 2003. Protein identification from 2-dimensional gel electrophoresis analysis of *Klebsiella pneumoniae* by combined use of mass spectrometry data and raw genome sequences. submitted.
- Welch RW, Rudolph FB, Papoutsakis ET. 1989. Purification and characterization of the NADH-dependent butanol dehydrogenase from *Clostridium acetobutyricum* (ATCC 824). *Archive Biochem Biophys* 273:309–318.
- Youngleson JS, Jones WA, Jones DT, Woods DR. 1989. Molecular analysis and nucleotide sequence of the *adh1* gene encoding an NADPH-dependent butanol dehydrogenase in the gram-positive anaerobe *Clostridium acetobutyricum*. *Gene* 78:355–364.
- Zeng AP, Biebl H. 2002. Bulk chemicals from biotechnology: The case of microbial production of 1,3-propanediol and the new trends. *Adv Biochem Eng Biotechnol* 74:237–257.